

Omnidirectional and compact guided light extraction from Archimedean photonic lattices

M. Rattier,^{a)} H. Benisty,^{b)} E. Schwoob, and C. Weisbuch

Laboratoire de Physique de la Matière Condensée, Ecole Polytechnique, F-91128 Palaiseau, France

T. F. Krauss^{c)} and C. J. M. Smith^{d)}

Optoelectronics Research Group, Glasgow University, Glasgow, G12 8LT Scotland

R. Houdré and U. Oesterle

Institut de Photonique et d'Electronique Quantique, Ecole Polytechnique Fédérale de Lausanne, CH-1015 Switzerland

(Received 20 January 2003; accepted 13 June 2003)

We address the issue of extracting light from a waveguide towards air in a compact way for randomly oriented guided waves. The goal is to enhance the extraction efficiency of light-emitting diodes while retaining planar processing. For incidence-angle-independent extraction, preferred lattice designs appear to possess a ring-shaped Fourier transform. We demonstrate this property for an Archimedean lattice. This system is the outer part of a resonant-cavity light-emitting diode. Data suggest that $\sim 40\%$ extraction efficiency is at hand in a planar top-emitting device retaining its substrate. © 2003 American Institute of Physics. [DOI: 10.1063/1.1600831]

Photonic crystals (PCs) exhibit band gaps or peculiar photon dispersions.¹ In two-dimensions (2D), most realizations have been based on triangular lattices of holes.² Investigation of quasicrystals has been prompted by the promise of larger band gaps,^{3–5} fractal density-of-states,⁶ or localized resonances.⁷ Quasiperiodicity has only found actual applications in one dimension (1D) in nonlinear optics,⁸ and not yet in 2D. We propose here to use these complex 2D lattices for omnidirectional light outcoupling off a planar waveguide, in view of semiconductor solid-state lighting. In light-emitting diodes (LEDs), extraction of guided light has been tackled using random lattices⁹ or triangular 2D PCs in their “air” band,¹⁰ or by “reshaping” the in-plane allowed directions.¹¹ These solutions affect compactness or brightness, or require substrate removal.

The extraction of guided waves through diffraction is a tricky problem: extracting around normal incidence a *monochromatic, collimated* guided light having a propagation constant k_{\parallel} (effective index $n_{\text{eff}} = k_{\parallel}c/\omega$ with usual notations) is easily achieved by a 1D lattice with grooves normal to the beam and periodicity $a \sim a_0 = 2\pi/k_{\parallel}$ (at first-order for extraction), all the more if one frustrates the second-order Bragg backreflection by detuning [Fig. 1(a)]. Extraction to air is allowed by the absence of k_{\perp} conservation in a thin film, and its amplitude maximized by a proper choice of hole shape (the form factor in diffraction theory). Unlike this simple situation, extraction from a LED demands acceptance for both spread in emission wavelength and incidence angles. Spectral deviations $\Delta\omega$ steer the air beam [change of k_{\parallel} in Fig. 1(a)] but the acceptance $\Delta\omega/\omega$ to remain extracted is of

the order, $1/n_{\text{eff}} \sim 0.3$. The spread in incidence angle in a LED is more challenging as the wave vector k_y along the groove has to be conserved, most of the guided waves, having an in-plane azimuth $\theta > \theta_{c,\text{eff}} = \sin^{-1}(1/n_{\text{eff}}) \sim 0.3$ rad are not extracted at all [Fig. 1(b)]. 2D PCs do not solve completely the issue: triangular PCs¹⁰ suffer from a similar limitation as their small period ($\sim \lambda/2n_{\text{eff}}$) provides at best a second extraction window for large θ 's [see later Fig. 3(f)], except for emission from unpractical micron-sized cavities,^{12,13} where confinement relaxes k_{\parallel} conservation.

We start from a microcavity-LED-type multilayer stack in which light emission occurs in a GaAs layer. The use of high index contrast GaAs/“ AlO_x ” Bragg mirrors [“ AlO_x ” of refractive index ~ 1.6 is obtained by lateral oxidation of high-Al content AlGaAs layer, Fig. 2(a)] leads to a high “vertical” extraction efficiency, up to a record of 29%.^{14,15} Of the 71% left in this example, 26% go into the substrate through leaky modes (TE or TM) and 45% go into the guided mode supported by the GaAs cavity.

Our goal is thus to extract as much as possible of the guided light reservoir before it is, e.g., laterally reabsorbed. Our guess is that extracting lattices (EL) suited to our scope

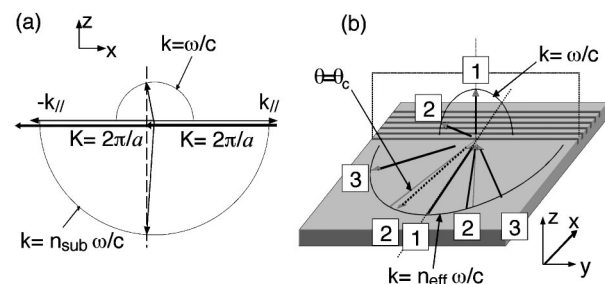


FIG. 1. (a) Extraction of a collimated guided beam in the substrate (bottom semicircle) and the air (upper semicircle); note the forbidden second-order reflection ($k_{\parallel} - 2K$ falls too far). (b) The limited angular extraction of a guided wave by a one-dimensional grating: waves (1) and (2) are extracted but a wave (3) impinging above a critical angle $\theta_{c,\text{eff}} = \sin^{-1}(1/n_{\text{eff}})$ is not.

^{a)}Present address: Luxtera Inc., Pasadena, California.

^{b)}Author to whom correspondence should be addressed; also at: Institut d'Optique, 91403 Orsay, France; electronic mail: henri.benisty@iota.u-psud.fr

^{c)}Present address: St Andrews University, School of Physics and Astronomy.

^{d)}Present address: Intense Photonics Ltd, Scotland.

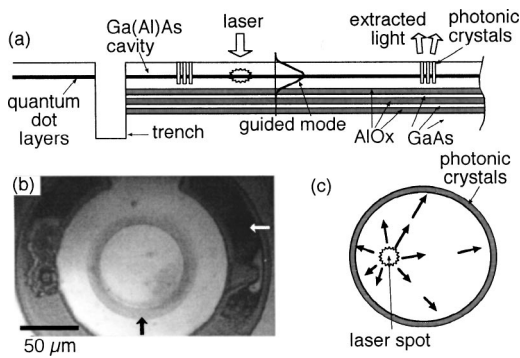


FIG. 2. Geometry of experiments: (a) side view; (b) top view micrograph; the white arrow is the trench while the black one is the photonic crystal (c) scheme of the experiment seen from top.

possess a “round,” ring-like Fourier transform $\varepsilon(k_{\parallel})$. We implemented such lattices, specifically Archimedean tilings,⁴ at the periphery of the emitting structure described earlier. The ring-like reciprocal space map favors single pass extraction and close to ultimate compacity (a few microns penetration in the lattice) crucial to high-brightness devices. The full prediction of a given EL is however a full-fledged three-dimensional (3D) electromagnetic issue. Taking a pragmatic view, the broad angular acceptance of the GaAs/ AlO_x bottom mirror minimizes radiation towards the substrate.

In our experiments, the stack is a GaAs “ λ ” cavity on top of the mirror [Fig. 2(a)], but being designed for photoluminescence experiments, it has only a peak 20% vertical extraction efficiency. The EL surrounds an 80 μm diameter emitting zone [Fig. 2(b)]. We focus at a chosen point in this zone a 678 nm laser with a lens [numerical aperture (NA)=0.4] to induce an internal guided light source from three InAs quantum dots (QDs) layers embedded in the GaAs layers [Figs. 2(a) and 2(c)]. QDs, deliberately grown with a broad size distribution, emit from 900 to beyond our 1060 nm detector cutoff. This vertical stack captures about 33% of the QD emission into its single TE guided mode. The modal absorption length, $\sim 50 \mu\text{m}$, allows most of guided photons to reach the periphery. Light imaged on a camera through the NA=0.4 lens is filtered at $\lambda=1052 \text{ nm}$ ($\Delta\lambda=14 \text{ nm}$) to isolate the EL quasimonochromatic properties.

The EL probed here are mapped around the 80 μm ring [Fig. 2(c)]: they have a “radial period” a_r while their “azimuthal period,” a_{θ} , increases by $\sim 0.5\%–1\%$ per row (we refer a_{θ} to the innermost ring value); all ELs feature round holes of diameter d , and depth 150–300 nm (due to the different structures studied; the detailed impact on extraction efficiency is not known. We define f as their air filling factor (e.g., $f = \pi d^2 / 4a_r a_{\theta}$ in a rectangular lattice). We first tested a quasi-1D rectangular lattice [Fig. 3(a)] with $a_r = 380 \text{ nm}$, and $a_{\theta} = 220 \text{ nm}$ (no in-plane diffraction allowed), $d = 140 \text{ nm}$, so that $f \sim 20\%$. It illustrates directional extraction [Fig. 1(b)]. Next, we probed a triangular lattice [Fig. 3(b)], ($\theta=0$ is the ΓK crystal direction), with a period $a = 500 \text{ nm}$ and $f = 55\%$. It illustrates a simple 2D crystal; the large f translate into a rather reflective behavior and a short propagation length in it. Finally, we implemented Archimedean tilings A7 and A13, with cells as described in Fig. 3(c);⁴ the 12 equivalent second neighbors of the cell’s central atom in A13 made are clear in Fig. 3(d). Results with

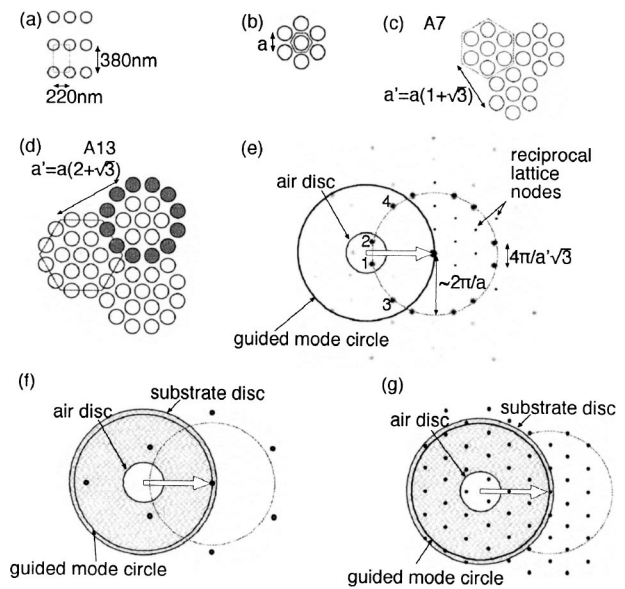


FIG. 3. (a)–(d) The three kinds of extracting lattices probed: quasi-1D lattice (a); triangular lattice (b); Archimedean lattices A7 (c) and A13 (d); (e) Ewald construction for light impinging on the A13 crystal, with the Fourier transform of its dielectric function shown as variable gray levels. Also plotted are the air disc and guided wave circle; similar construction for (f) the triangular lattice of (b) and (g) for a generic large period lattice.

nearest-neighbor-distances (NND) of 500 and 550 nm are discussed here.

For *directional* extraction measurements of each EL, excitation is focused off-center by $\sim 20 \mu\text{m}$ (Fig. 4, when excited in their center, all EL display a uniform extraction). To measure the extraction efficiency, we convolve the intensity map $I_{\text{ext}}(\alpha_0, r)$ at polar angle α_0 by the function $g(r, \alpha) = \exp\{-[(r-R)^4 + R^4(\alpha - \alpha_0)^4] / b^4\}$ ($b \sim 4 \mu\text{m}$). The spot center is found directly from the captured picture [Fig. 4(a)]. Then, the angle of incidence (denoted θ) and guided light path r' are determined [Fig. 4(b)]. The source extent introduces a convolution which is far more severe on the closer side, not shown here. In this way, measurement of extraction for θ from 0° to 60° is obtained from a single image capture, without calibration problems. Finally, the data $I_{\text{ext}}(\theta)$ are

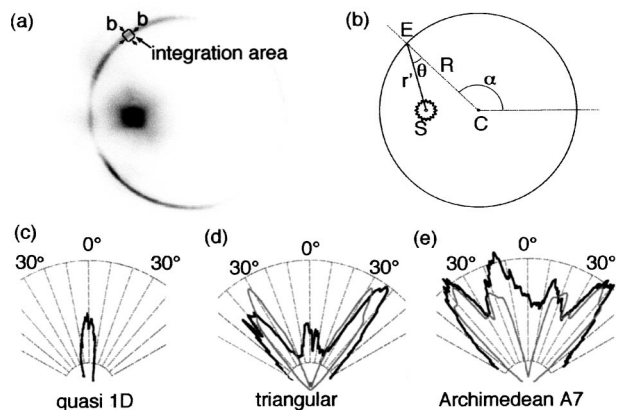


FIG. 4. (a) Typical image analyzed; (b) angles α and in-plane incidence angle θ ; (c)–(e) polar plot (thick lines) of extraction profiles $I_{\text{ext}}(\theta)$ for: (c) quasi-1D lattice; (d) triangular lattice; (e) Archimedean lattices A7. Thin smoother lines in (d) and (e) are from the kinematic diffraction model of Ref. 16. Radial scale for (c) is ten times that for (d) and (e); for that particular sample, hole size was optimum, unlike (d) and (e); see Figs. 3(a)–3(c) for the different fill factors.

corrected from a factor $r'/\cos\theta$, accounting for divergence of guided waves and the oblique power flux effect. We neglected absorption, a factor of 2 at most.

The extraction profiles $I_{\text{ext}}(\theta)$ are shown in Figs. 4(c)–4(e) on polar plots. Figure 4(c) relates to the quasi-1D EL. Its single peak width indicates an internal angle resolution $\Delta\theta = 15^\circ$. The capturing aperture $\text{NA}=0.4$ accounts for $\sin^{-1}(\pm\text{NA}/n_{\text{eff}})\sim\pm 6^\circ$ which adds to the $4\ \mu\text{m}$ source extent at $r'=65\ \mu\text{m}$ from the EL, $[\tan^{-1}(4/65)\sim 3.5^\circ]$. Figure 4(d) gives $I_{\text{ext}}(\theta)$ for the 500 nm period triangular lattice, with two strong diffraction peaks around $\theta=38^\circ$ (larger periods just give smaller θ 's). Finally, Fig. 4(e) shows $I_{\text{ext}}(\theta)$ for A7 and $\text{NND}=550\ \text{nm}$ (A13 and $\text{NND}=500\ \text{nm}$ gives about similar results). Peak angles in Figs. 4(d)–4(e) are well accounted by a basic kinematic diffraction model¹⁶ treating the EL holes as point scatterers illuminated by a plane guided wave.

In striking contrast to previous cases, the new lattices, e.g., A7 efficiently extract over a wide range of angles θ . One could argue that this would be the case for any large period EL, with a sufficiently small mesh in k space to be merged within $\Delta\theta$. The best answer is quantitative: Let γ be the areal scaling factor of the new EL ($\gamma=7$ for A7, 13 for A13). A triangular EL with an enlarged period by the factor $\gamma^{1/2}$ would allow γ times more channels for diffraction out of the guide [similar to the difference between Figs. 3(f) and 3(g)]. The emission into any of these channels would be divided by γ , and furthermore, most of them would radiate towards the substrate, not towards air, since related wavevectors would almost evenly sample k space [Fig. 3(g)]. It is clear that the extracted peaks in Fig. 4(e) are not weaker than in Fig. 4(d), but more numerous. The reason for this can be traced to the ring-like Fourier transform $\varepsilon(k)$ of the Archimedean lattice dielectric map [Fig. 3(e)]: unlike a standard lattice in which the strength of the peaks (the atom form factor of x-ray diffraction) oscillates and decays with the modulus of k , the peculiar arrangement of the Archimedean tilings cancels most of the unwanted channels and concentrates radiation in desired ones on the ring of k_{\parallel} . Let us discuss the A7 lattice [Fig. 3(e)]. We represent two concentric disks for the air and guided mode circles, and make the usual Ewald construction of kinematic diffraction. For this $\gamma=7$ example ($\theta=0$), two principal spots lie in the air disk, and the crucial point is that there will be always “principal” spots (i.e., reinforced by the Archimedean structure factor) in the air disk when θ changes. Compare to the triangular lattice, Fig. 3(f). The reciprocal lattice vectors of A7 in the extracting windows towards air or substrate are very few, numbered 1 and 2 (3 and 4), respectively, hence an extraction efficiency of guided light to air in the 50% range. Whether higher γ would be better is unclear, as denser lattice points will saturate the extraction efficiency at the ratio of the circle arcs for air and substrate diffraction. We can evaluate the absolute extraction efficiency of the Archimedean lattice by comparing the angle-integrated intensity diffracted by the EL to the inten-

sity directly emitted in the vertical direction from the excited spot. This then leads to an EL extraction efficiency of the order of 10%.¹⁴ More knowledge and 3D simulations are needed to take full advantage of these Archimedean EL, the main issues being the role of the underlying mirror in minimizing substrate radiation by forming a weak cavity with the semiconductor/air interface, the reduction of in-plane reflection, and the overall brightness optimization.

As of today, the association of microcavity effects, with overall efficiencies up to 29%¹⁵ and of Archimedean PC extractors can be foreseen to lead to over 40% efficiency in air in a full planar process, and significantly more for devices with transparent substrates, as is the case for nitride and advanced GaAlInP LEDs, as then the substrate radiation is not lost. It should be remarked in addition that as the diffraction occurs over a few lattice periods only, the extractor has a high local brightness, similar to that of the central microcavity area. In conclusion, we firmly conjecture that lattices with ring-like $\varepsilon(k)$ distributions are unavoidable to optimally achieve the desired omnidirectional extraction in PC-assisted LEDs. Specifically, we used Archimedean lattices for this purpose. Our data show that extraction of guided light from different in-plane angles takes place evenly, with clear indications that this effect was not obtained to the expense of extraction efficiency.

¹ See feature section in IEEE J. Quantum Electron. **38**, 724 (2002).

² H. Benisty, M. Rattier, and S. Olivier, C.R. Physique **3**, 89 (2002).

³ P. L. Hagelstein and D. R. Denison, Opt. Lett. **54**, 708 (1999).

⁴ S. David, A. Chelnokov, and J.-M. Lourtioz, Opt. Lett. **25**, 1001 (2000).

⁵ M. E. Zoorob, M. D. B. Charlton, G. J. Parker, J. J. Baumberg, and M. C. Netti, Nature (London) **404**, 740 (2000).

⁶ T. F. Krauss, B. Vogebe, C. R. Stanley, and R. M. De La Rue, IEEE Photonics Technol. Lett. **9**, 176 (1997).

⁷ E. Özbay and B. Temelkuran, Appl. Phys. Lett. **69**, 743 (1996).

⁸ S. N. Zhu, Y. Y. Zhu, and M. B. Ming, Science **278**, 843 (1997).

⁹ R. Windisch, P. Heremans, A. Knobloch, P. Kiesel, G. H. Döhler, B. Dutta, and G. Borghs, Appl. Phys. Lett. **74**, 2256 (1999).

¹⁰ M. Boroditsky, T. F. Krauss, R. Coccioli, R. Vrijen, R. Bhat, and E. Yablonovitch, Appl. Phys. Lett. **75**, 1036 (1999).

¹¹ A.-L. Fehrembach, S. Enoch, and A. Sentenac, Appl. Phys. Lett. **79**, 4280 (2001).

¹² S. Fan, P. R. Villeneuve, and J. D. Joannopoulos, Phys. Rev. Lett. **78**, 3294 (1997).

¹³ See, e.g., C. J. M. Smith, T. F. Krauss, H. Benisty, M. Rattier, C. Weisbuch, U. Oesterle, and R. Houdré, J. Opt. Soc. Am. B **17**, 2043 (2000); C. Reese, C. Becher, A. Imamoglu, E. Hu, B. D. Gerardot, and P. M. Petroff, Appl. Phys. Lett. **78**, 2279 (2001); T. Yoshie, J. Vuckovic, A. Scherer, H. Chen, and D. Deppe, *ibid.* **79**, 4289 (2001).

¹⁴ M. Rattier, Ph.D. dissertation, Ecole Polytechnique, France, 2002.

¹⁵ M. Rattier, H. Benisty, R. Stanley, J.-F. Carlin, R. Houdré, U. Oesterle, C. J. M. Smith, C. Weisbuch, and T. F. Krauss, IEEE J. Sel. Top. Quantum Electron. **8**, 238 (2002).

¹⁶ We use for a kinematic diffraction model towards air the same approach as in the appendix A of the paper by Smith *et al.*, J. Opt. Soc. Am. B. Here the field is scalar and propagates in the EL with an index $n=2.1$ ($f=55\%$). The scatterers are point like (no azimuthal form factor), hence, the integral of the mentioned appendix becomes a discrete sum over the holes located at \mathbf{r}_j of the common form $\sum \exp(i\Delta\mathbf{k}\cdot\mathbf{r}_j)$ in diffraction theory. Also, the degraded angular resolution is accounted for by a square $\pm 6^\circ$ convolution over θ , and an attenuation of $1\ \mu\text{m}^{-1}$ is assumed when penetrating the EL to account for depletion by radiation losses.